Quantum imaging with incoherently scattered X-rays from a Free-Electron Laser

Joachim von Zanthier

Quantum Optics and Quantum Information,
Institute of Optics, Information and Photonics,
University of Erlangen-Nuremberg, Germany

Workshop "Frontiers of X-rays in the Physical Sciences", Imperial College, London, 13.11.2019

Quantum imaging with incoherently scattered X-rays from a Free-Electron Laser

I. Imaging with coherently diffracted vs. incoherently scattered light:

Young interference, Hanbury Brown Twiss measurement & higher order photon correlations

II. Imaging of arbitrary 1D and 2D source distributions with FLASH at XUV wavelengths using higher order photon correlations

III. Outlook:

Incoherent Diffraction Imaging (IDI) of 3D atomic source distributions with hard X-rays

I. Young, Hanbury-Brown Twiss, & higher order photon correlations

Young's double slit : wave description

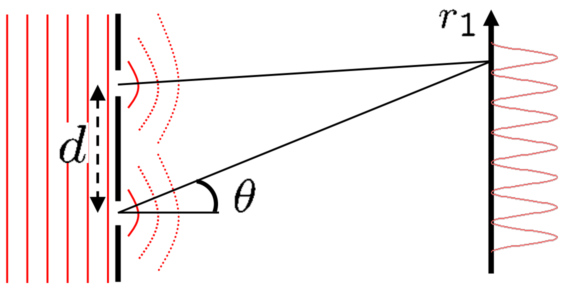

Intensity distribution:

$$I(r_1) = \langle E^\star(r_1)\, E(r_1)\rangle = G^{(1)}(r_1)$$

$$I(r_1) \propto 1 + \cos(kd\sin\theta)$$

Th. Young (1773 – 1829)

Young's double slit : quantum path description

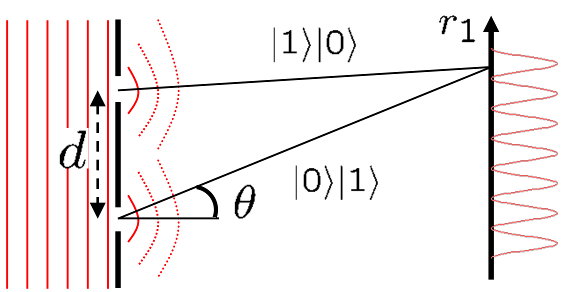

$$\boxed{|\phi\rangle = \frac{1}{\sqrt{2}}\left(|1\rangle|0\rangle + e^{i\Phi}|0\rangle|1\rangle\right)}$$

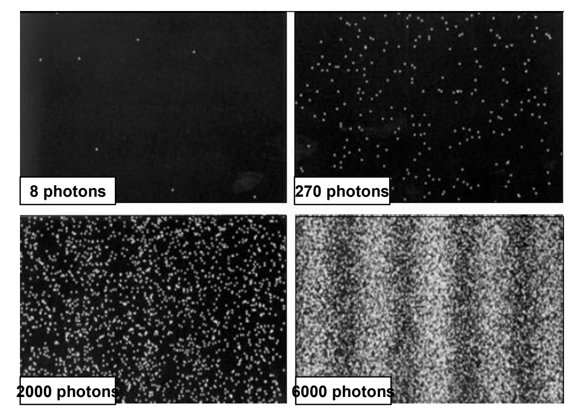

Dirac: "Each photon interferes only with itself.
Interference between two different photons never occurs."

I. Young, Hanbury-Brown Twiss, & higher order photon correlations

Young's double slit experiment with single atoms

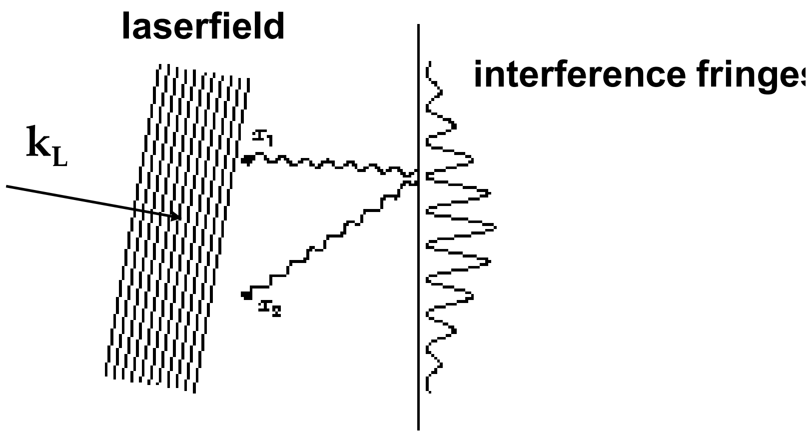

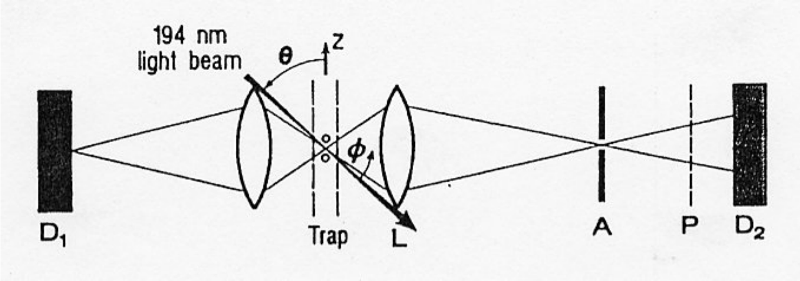

U. Eichmann et al., PRL 70, 2359 (1993)

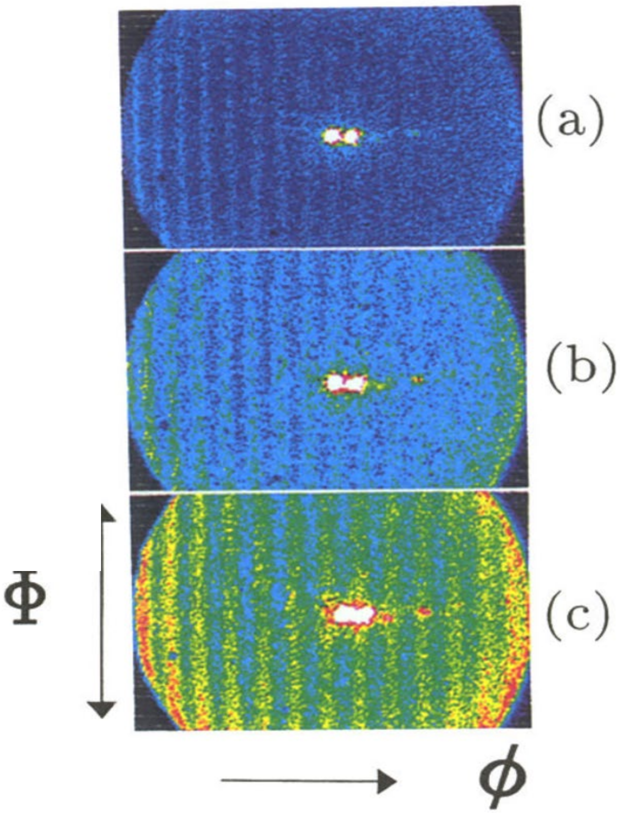

FIG. 2. Interference pattern for three different ion separations: (a) 5.4 μm, (b) 4.3 μm, and (c) 3.7 μm. The two white spots are caused by stray reflections of the laser beam.

I. Young, Hanbury-Brown Twiss, & higher order photon correlations

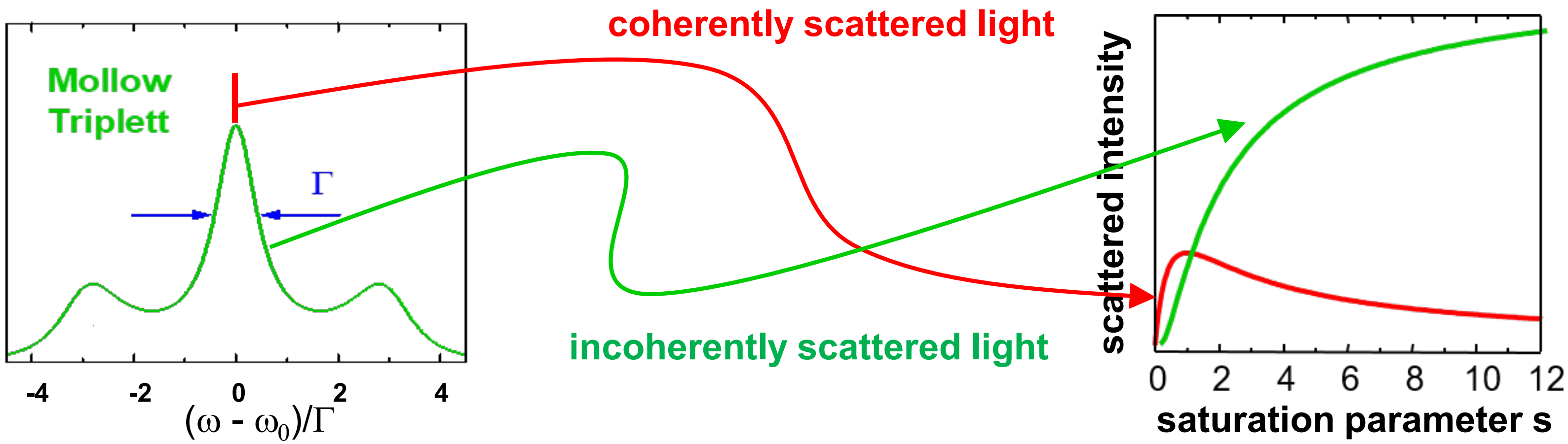

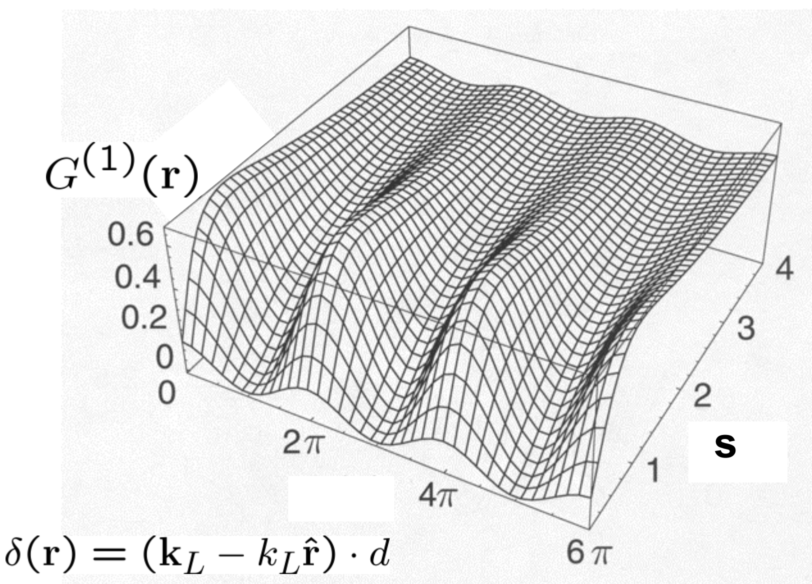

steady state

$$\boxed{\mathcal{V} = \frac{1}{1+s} \xrightarrow{s\to\infty} 0}$$

Itano et al., PRA 57, 4176 (1998)
Skornia, JvZ, Agarwal, Werner, Walther, PRA 64, 063801 (2001)

I. Young, Hanbury-Brown Twiss, & higher order photon correlations

Young's double slit experiment with two atoms in excited state $|e, e\rangle$

spontaneous decay $\longrightarrow$ incoherent emission of radiation

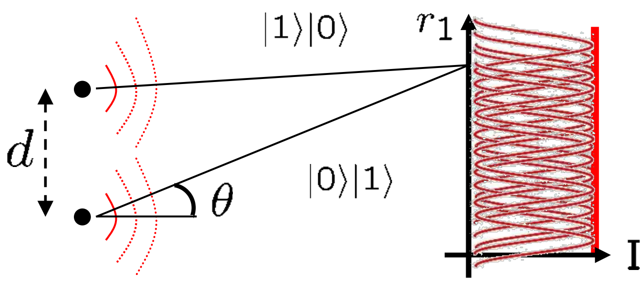

$$|\phi\rangle = \frac{1}{\sqrt{2}}\left(e^{i\Phi_1}|1\rangle|0\rangle + e^{i\Phi_2}|0\rangle|1\rangle\right)$$

$\longrightarrow$ no interference fringes in $G^{(1)}$

two atoms in state $|e, e\rangle$

with $\quad \hat{E}^{(+)}(\vec{r}_j) \sim \sum_{l=1}^{2} e^{-i\,\Phi_{lj}}\,\hat{s}_l^- \quad$ and $\quad \hat{s}_l^- = |g\rangle_l\langle e|$

$$G^{(1)}(\mathbf{r}_1) = \langle e, e\,|\,\mathbf{E}^{(-)}(\mathbf{r}_1)\,\mathbf{E}^{(+)}(\mathbf{r}_1)\,|e, e\rangle \;\sim\; const.$$

I. Young, Hanbury-Brown Twiss, & higher order photon correlations

Hanbury-Brown Twiss measurement for two atoms in state $|e, e\rangle$

double star

Hanbury BrownTwiss, Nature 177, 27 (1956)
Hanbury BrownTwiss, Nature 178, 1046 (1956)
Hanbury Brown, Nature 218, 637 (1968)

Photon-photon-correlation of fluorescence light of two atoms

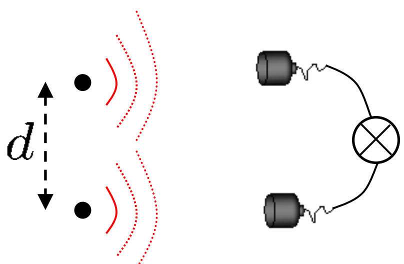

$$G^{(2)}(r_1, r_2) \sim \langle E^-(r_1)\, E^-(r_2)\, E^+(r_2)\, E^+(r_1) \rangle$$

I. Young, Hanbury-Brown Twiss, & higher order photon correlations

➡ Hanbury-Brown Twiss measurement for two atoms in state $|e, e\rangle$

$$G^{(2)}(\mathbf{r}_1; \mathbf{r}_2) = \langle e, e\,|\mathbf{E}^{(-)}(\mathbf{r}_1)\,\mathbf{E}^{(-)}(\mathbf{r}_2)\,\mathbf{E}^{(+)}(\mathbf{r}_2)\,\mathbf{E}^{(+)}(\mathbf{r}_1)\,|e, e\rangle$$

$$\boxed{= 1 + \cos[kd(\sin\theta_2 - \sin\theta_1)]}$$

two 2-level atoms

Two different quantum paths contribute to same final state:

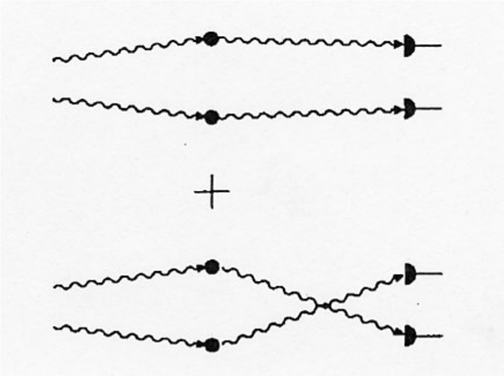

$$|e, e\rangle\,|0, 0\rangle \nearrow |g, e\rangle\,|1, 0\rangle \searrow |g, g\rangle\,|1, 1\rangle$$

$$|e, e\rangle\,|0, 0\rangle \searrow |e, g\rangle\,|1, 0\rangle \nearrow |g, g\rangle\,|1, 1\rangle$$

→ **interference fringes in $G^{(2)}$ expected**

Skornia, JvZ, Agarwal, Werner, Walther, PRA 64, 063801 (2001)
Agarwal, JvZ, Skornia, Walther, PRA 65, 053826 (2002)

I. Young, Hanbury-Brown Twiss, & higher order photon correlations

Higher order photon correlation functions:

$$G^{(2)}(\mathbf{r}_1, \mathbf{r}_2) = \langle \hat{E}^{(-)}(\mathbf{r}_1)\, \hat{E}^{(-)}(\mathbf{r}_2)\, \hat{E}^{(+)}(\mathbf{r}_2)\, \hat{E}^{(+)}(\mathbf{r}_1) \rangle$$

R. J. Glauber

Phys. Rev. 130, 2529 (1963);
ibid. 131, 2766 (1963)
Nobel prize 2005

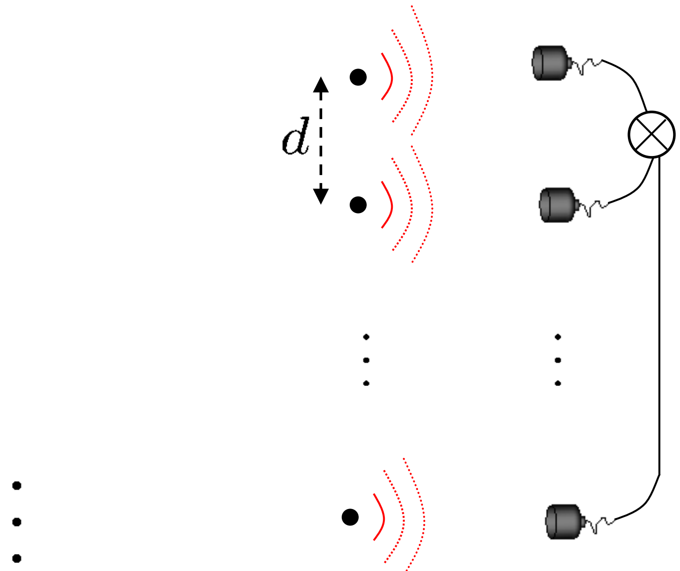

$$G_N^{(m)}(\mathbf{r}_1, \ldots, \mathbf{r}_m) = \langle \hat{E}^{(-)}(\mathbf{r}_1) \ldots \hat{E}^{(-)}(\mathbf{r}_m) \hat{E}^{(+)}(\mathbf{r}_m) \ldots \hat{E}^{(+)}(\mathbf{r}_1) \rangle$$

→ **can be used for improved imaging?**

Quantum imaging with incoherently scattered light from a Free-Electron Laser

I. Imaging with coherently diffracted vs. incoherently scattered light:

Young interference, Hanbury Brown Twiss measurement & higher order photon correlations

II. Imaging of arbitrary 1D and 2D source distributions with FLASH at XUV wavelengths using higher order photon correlations

III. Outlook: Incoherent Diffraction Imaging (IDI) of 3D atomic source distributions using hard X-rays

II. Quantum imaging arbitrary 1D and 2D source distribution in the XUV

N incoherent light sources (TLS) on a 1D grid with lattice constant d

$$x_l \in \mathbb{N}$$

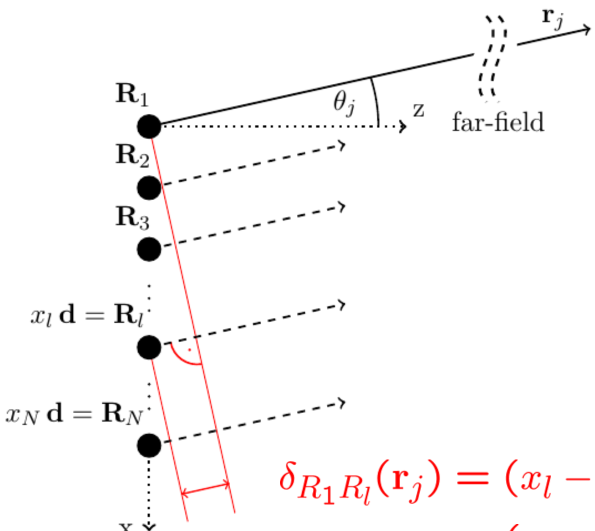

$$\delta_{R_1 R_l}(\mathbf{r}_j) = (x_l - x_1)kd\sin\theta_j$$
$$= (x_l - x_1)\delta_j$$

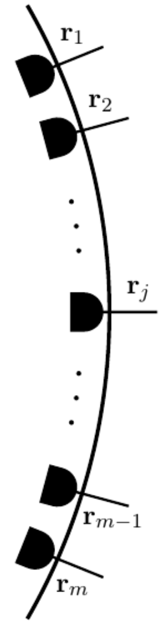

***m* detectors in the far-field**

$$\hat{E}^{(+)}(\mathbf{r}_j) = \sum_{l=1}^{N} \hat{E}_l^{(+)}(\mathbf{r}_j) \propto \sum_{l=1}^{N} e^{i\varphi_{R_l,j}}\hat{a}_l$$

$$\varphi_{R_l,j} \equiv k\frac{\mathbf{r}_j\cdot\mathbf{R}_l}{r_j} = x_l\,kd\sin(\theta_j) = x_l\,\delta_j$$

$$\boxed{g^{(m)}_{N\,\mathrm{TLS}}(\mathbf{r}_1,\ldots,\mathbf{r}_m) = \frac{\langle I(\mathbf{r}_1)\ldots I(\mathbf{r}_m)\rangle}{\langle I(\mathbf{r}_1)\rangle\ldots\langle I(\mathbf{r}_m)\rangle} = g^{(m)}_{N\,\mathrm{TLS}}(\delta_1,\ldots,\delta_m)}$$

II. Quantum imaging arbitrary 1D and 2D source distribution in the XUV

Detection scheme to determine F in 1D:

Magic positions for m-1 fixed det.

$$\delta_j = 2\pi \frac{j-2}{m-1} \quad \text{for} \quad j = 2, ..., m$$

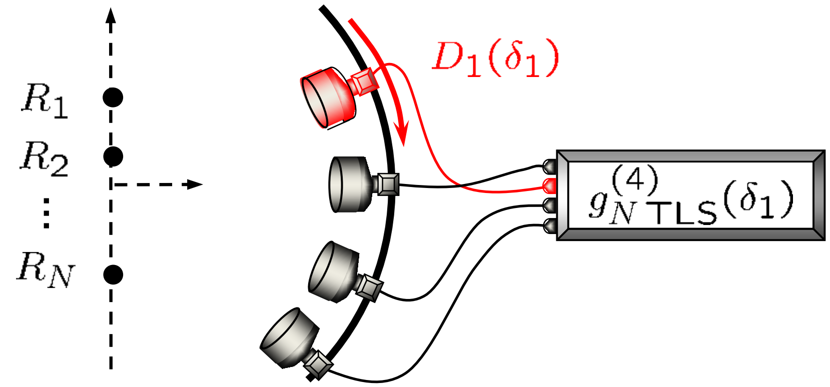

One moving detector $\Rightarrow g_N^{(m)}(\delta_1)$

Spatial frequency filtering:

$$g_N^{(m)}(\delta_1) = A_0^{(m)} + \sum_{\substack{a,l=1 \\ a \neq l}}^{N} A_{la}^{(m)} \cdot \begin{cases} \cos((x_l - x_a) \cdot \delta_1) & \text{if} \quad (x_l - x_a) \in \mathbb{N}_0 \cdot (m-1) \\ 0 & \text{else} \end{cases}$$

➡ only particular spatial frequencies appear within a given correlation order m

➡ m > 2: resolution below the Abbe limit

Classen, Waldmann, Giebel, Schneider, Bhatti, Mehringer, JvZ, PRL 117, 253601 (2016)

II. Quantum imaging arbitrary 1D and 2D source distribution in the XUV

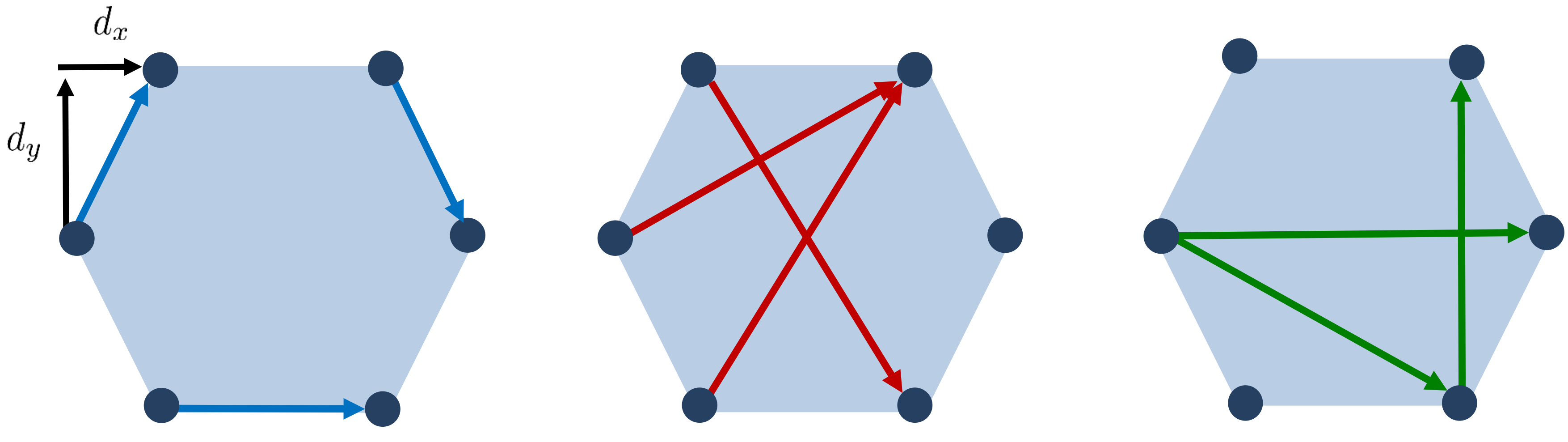

$\begin{pmatrix} 1 \\ 1 \end{pmatrix} \begin{pmatrix} 1 \\ -1 \end{pmatrix} \begin{pmatrix} 2 \\ 0 \end{pmatrix}$ $\quad$ $\begin{pmatrix} 2 \\ 2 \end{pmatrix} \begin{pmatrix} 2 \\ -2 \end{pmatrix} \begin{pmatrix} 3 \\ 1 \end{pmatrix}$ $\quad$ $\begin{pmatrix} 3 \\ -1 \end{pmatrix} \begin{pmatrix} 4 \\ 0 \end{pmatrix} \begin{pmatrix} 0 \\ 2 \end{pmatrix}$

Set of spatial frequencies

- **source geometry can be described on a grid with basis** $\begin{pmatrix} d_x \\ d_y \end{pmatrix} = \begin{pmatrix} \sqrt{3} \\ 1 \end{pmatrix} a$
- **Set of spatial frequencies F consists of 9 different spatial frequency vectors**

→ **Knowing F allows to determine the source distribution**

II. Quantum imaging arbitrary 1D and 2D source distribution in the XUV

Detection scheme to determine F:

- **m-1 fixed detectors located at *magic positions* (MP)**

along x-axis $\boxed{\delta_{j,x} = 2\pi \frac{j-2}{m-1} \quad \text{for} \quad j = 2, \ldots, m}$

- **one moving detector D_1 in the x-y-plane**

$$\Rightarrow g_N^{(m)}(\delta_{1,x}, \delta_{1,y}, MP_x)$$

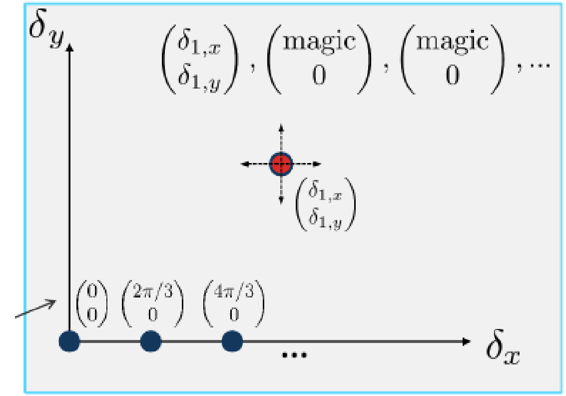

detector plane

Spatial frequency filtering:

$$g_N^{(m)}(\delta_{1,x}, \delta_{1,y}, MP_x) = A_0 + \sum_{\substack{a,l=1\\ a\neq l}}^{N} A_{la} \cdot \begin{cases} \cos\left[(x_l - x_a)\delta_{1,x} + (y_l - y_a)\delta_{1,y}\right] & \text{if } (x_l - x_a) \in \mathbb{Z}\cdot(m-1) \\ 0 & \text{else} \end{cases}$$

- **For m-1 fixed detectors at MP along x-axis: Filtering of 2D spatial frequencies, depending on correlation order m and x-component of spatial frequency**
- **Analogue filtering conditions for m-1 fixed detectors at MP along y-axis**

II. Quantum imaging arbitrary 1D and 2D source distribution in the XUV

Detection scheme to determine F:

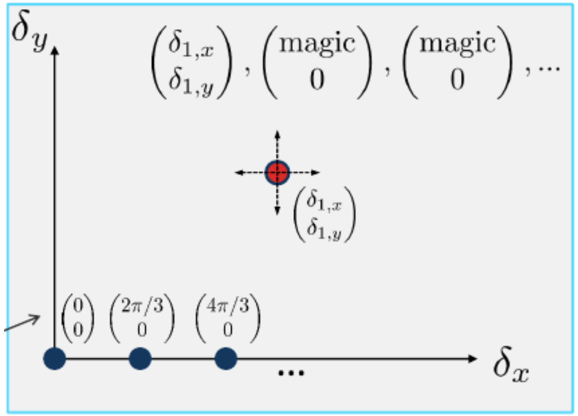

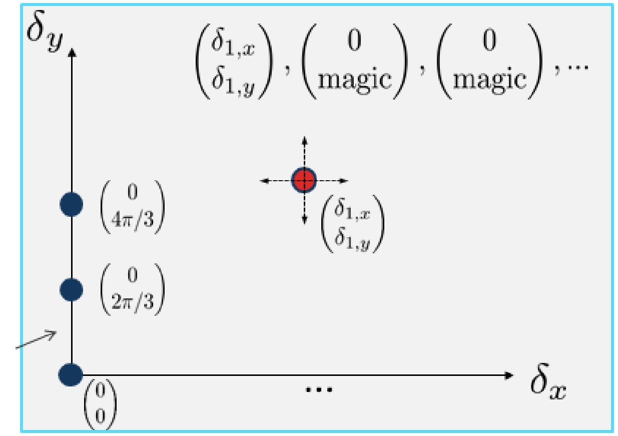

Detector plane

- **Measure $g^{(m)}(\delta_{1,x}, \delta_{1,y}, MP_x)$ for m = 3, 4, ... , with m-1 fixed detectors at MP_x**
- **Measure $g^{(m)}(\delta_{1,x}, \delta_{1,y}, MP_y)$ for m = 3, 4, ... , with m-1 fixed detectors at MP_y**

- **Measuring sequentially $g^{(m)}(\delta_{1x}, \delta_{1y}, MP_x)$ and $g^{(m)}(\delta_{1x}, \delta_{1y}, MP_y)$ for m > 2 enables determination of complete set of different spatial frequencies F**

II. Quantum imaging arbitrary 1D and 2D source distribution in the XUV

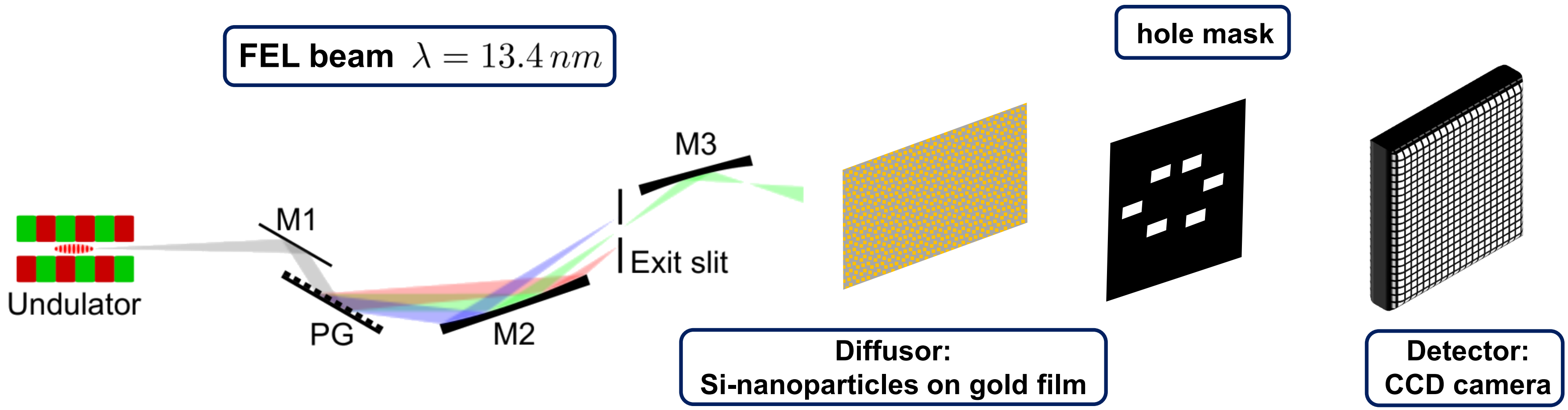

FLASH at DESY, Hamburg

N **artificial incoherent sources on a 2D-grid (with lattice constant d_x and d_y) using 6 holes arranged in form of a benzene molecule**

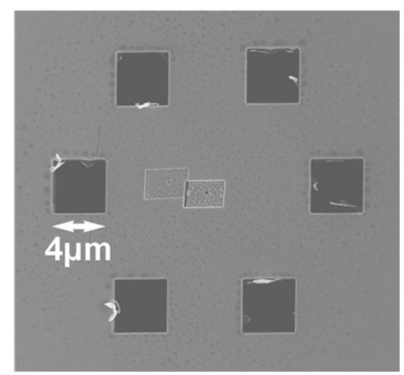

REM-image

II. Quantum imaging arbitrary 1D and 2D source distribution in the XUV

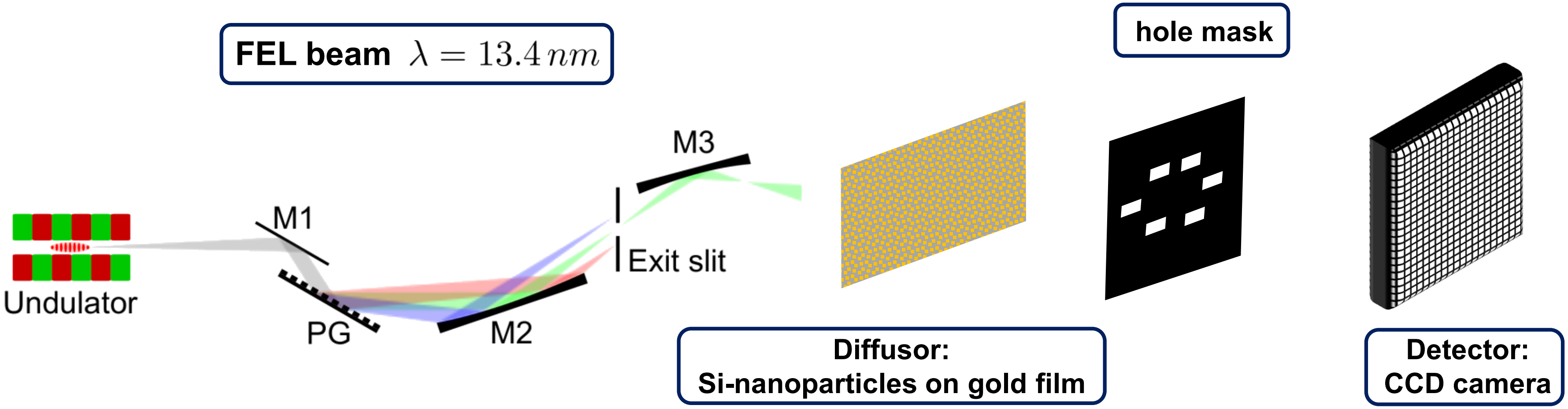

Experimental results: **10,000 images:**

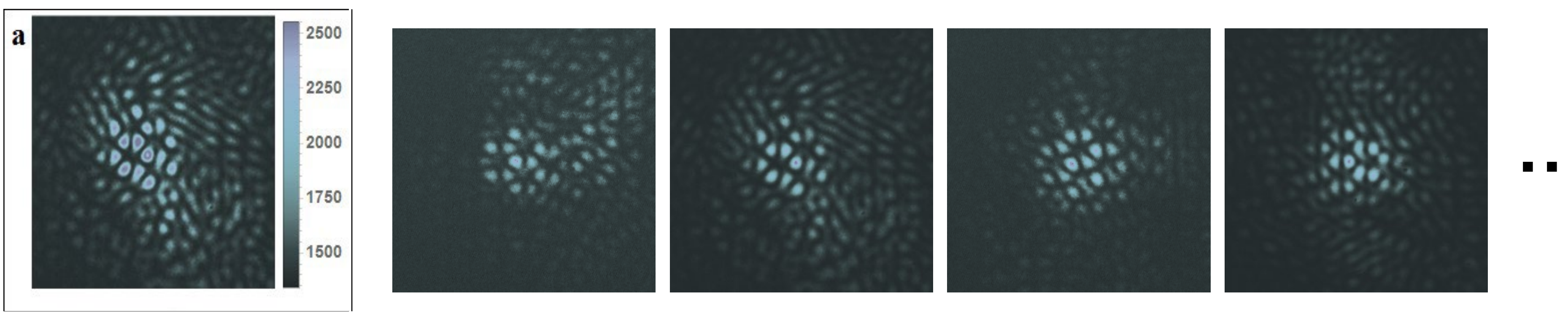

II. Quantum imaging arbitrary 1D and 2D source distribution in the XUV

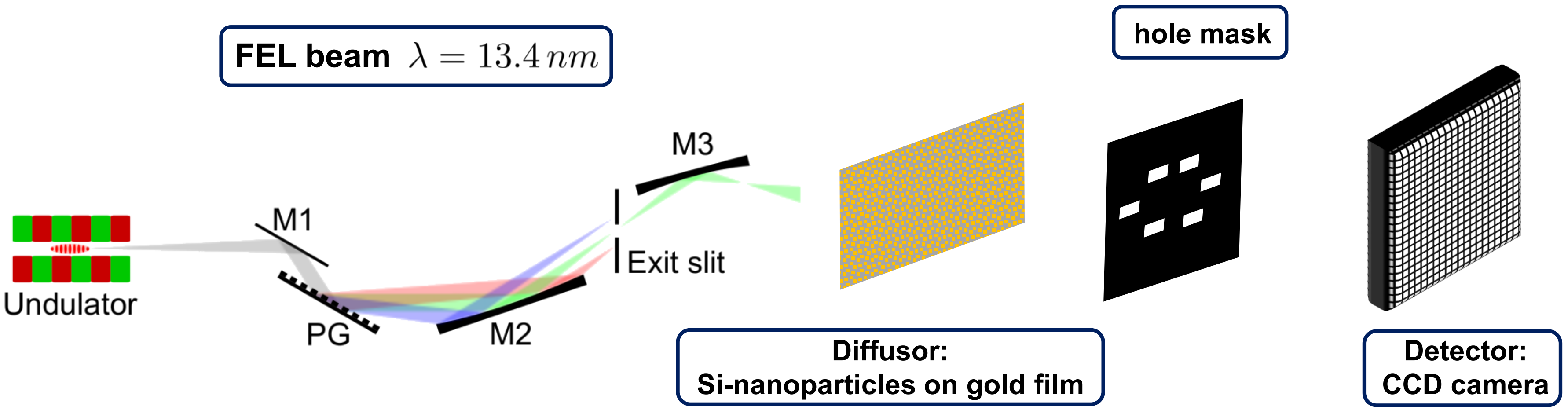

Experimental results: Example $g^{(4)}(\delta_{1,x}, \delta_{1,y}, MP_x)$

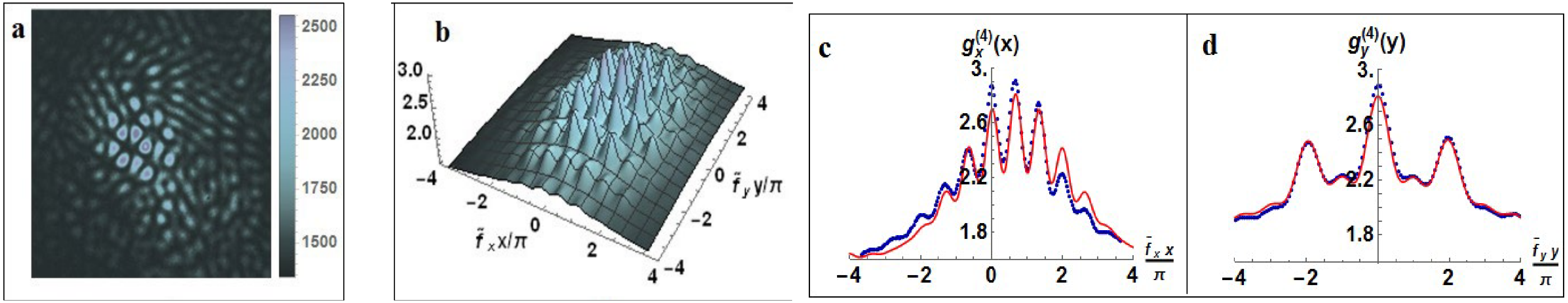

II. Quantum imaging arbitrary 1D and 2D source distribution in the XUV

Detection scheme to determine F:

REM Image

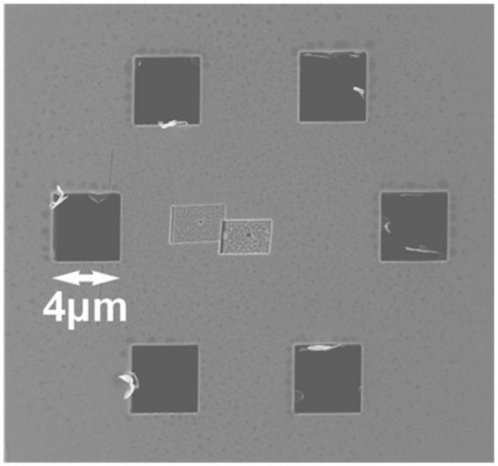

=

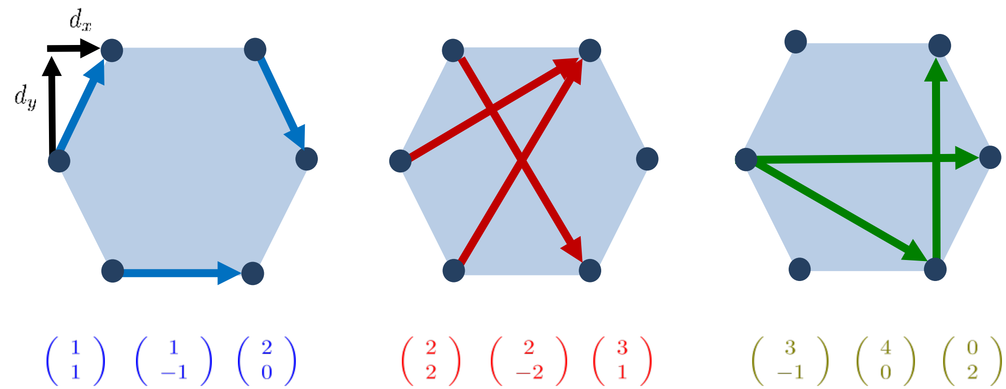

Result for F:

F	$\begin{pmatrix}1\\1\end{pmatrix}$	$\begin{pmatrix}1\\-1\end{pmatrix}$	$\begin{pmatrix}2\\0\end{pmatrix}$	$\begin{pmatrix}2\\2\end{pmatrix}$	$\begin{pmatrix}2\\-2\end{pmatrix}$	$\begin{pmatrix}3\\1\end{pmatrix}$	$\begin{pmatrix}3\\-1\end{pmatrix}$	$\begin{pmatrix}4\\0\end{pmatrix}$	$\begin{pmatrix}0\\2\end{pmatrix}$
$\mathbf{F_{exp}}$			$\begin{pmatrix}1.94\\0.02\end{pmatrix}$	$\begin{pmatrix}1.96\\2.00\end{pmatrix}$	$\begin{pmatrix}1.97\\-1.95\end{pmatrix}$	$\begin{pmatrix}2.97\\0.97\end{pmatrix}$	$\begin{pmatrix}2.97\\-1.03\end{pmatrix}$	$\begin{pmatrix}3.90\\0.04\end{pmatrix}$	$\begin{pmatrix}0.01\\1.98\end{pmatrix}$

Schneider, Mehringer, Mercurio, Wenthaus, Classen, Brenner, Gorobtsov, Benz, Bhatti, Bocklage, Fischer, Lazarev, Obukhov, Schlage, Skopintsev, Wagner, Waldmann, Willing, Zaluzhnyy, Wurth, Vartanyants, Röhlsberger, von Zanthier,
Nature Phys. 14, 126 (2018)

II. Quantum imaging arbitrary 1D and 2D source distribution in the XUV

Reconstructed Image of Source Distribution:

REM Image

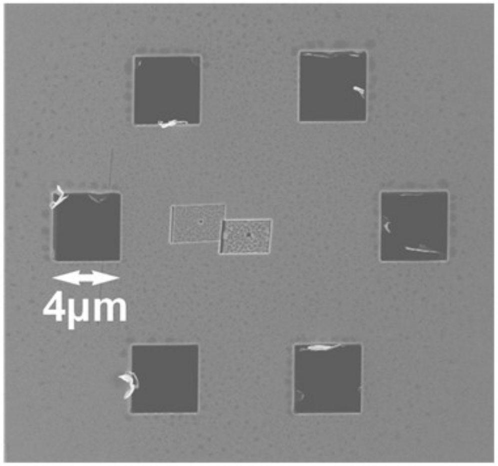

F

Reconstructed Image

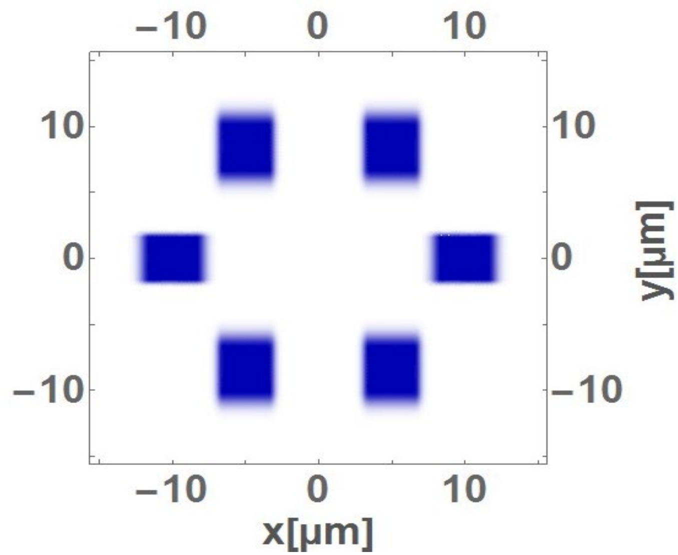

Result for F:

F	$\begin{pmatrix}1\\1\end{pmatrix}$	$\begin{pmatrix}1\\-1\end{pmatrix}$	$\begin{pmatrix}2\\0\end{pmatrix}$	$\begin{pmatrix}2\\2\end{pmatrix}$	$\begin{pmatrix}2\\-2\end{pmatrix}$	$\begin{pmatrix}3\\1\end{pmatrix}$	$\begin{pmatrix}3\\-1\end{pmatrix}$	$\begin{pmatrix}4\\0\end{pmatrix}$	$\begin{pmatrix}0\\2\end{pmatrix}$
$\mathbf{F}_{\mathbf{exp}}$			$\begin{pmatrix}1.94\\0.02\end{pmatrix}$	$\begin{pmatrix}1.96\\2.00\end{pmatrix}$	$\begin{pmatrix}1.97\\-1.95\end{pmatrix}$	$\begin{pmatrix}2.97\\0.97\end{pmatrix}$	$\begin{pmatrix}2.97\\-1.03\end{pmatrix}$	$\begin{pmatrix}3.90\\0.04\end{pmatrix}$	$\begin{pmatrix}0.01\\1.98\end{pmatrix}$

Schneider, Mehringer, Mercurio, Wenthaus, Classen, Brenner, Gorobtsov, Benz, Bhatti, Bocklage, Fischer, Lazarev, Obukhov, Schlage, Skopintsev, Wagner, Waldmann, Willing, Zaluzhnyy, Wurth, Vartanyants, Röhlsberger, JvZ,
Nature Phys. 14, 126 (2018)

II. Quantum imaging arbitrary 1D and 2D source distribution in the XUV

Reconstructed Image of Source Distribution:

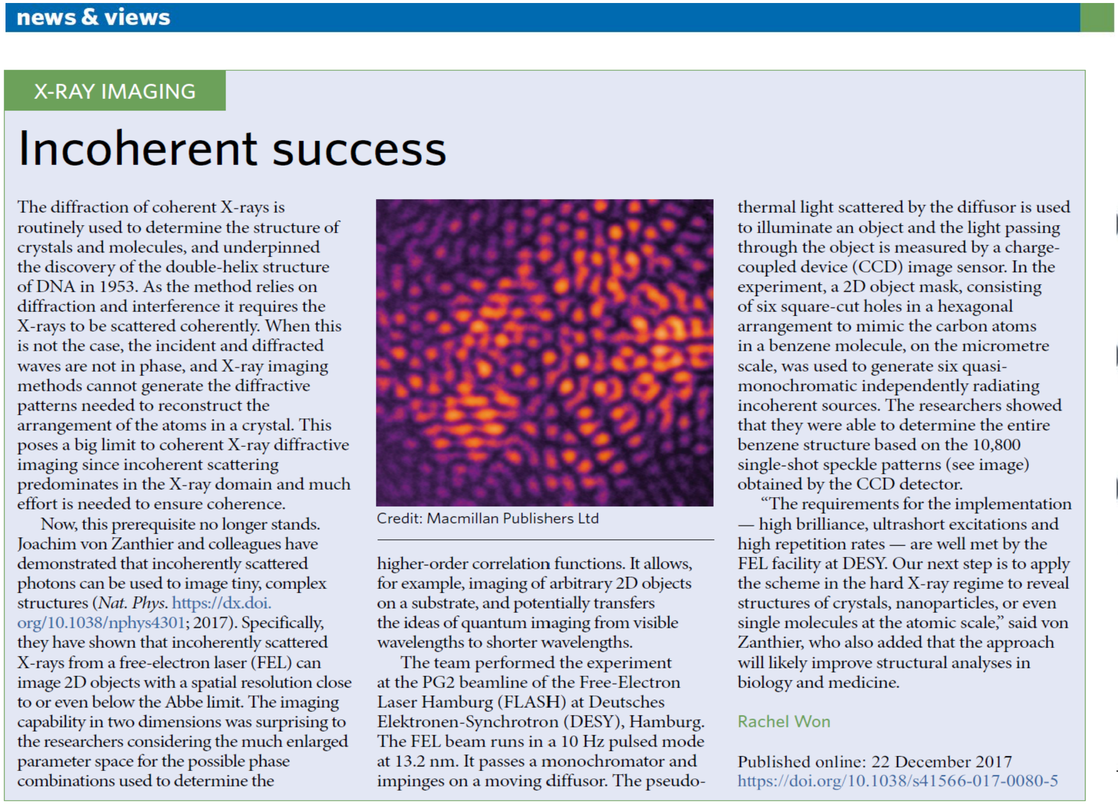

news & views

X-RAY IMAGING

Incoherent success

The diffraction of coherent X-rays is routinely used to determine the structure of crystals and molecules, and underpinned the discovery of the double-helix structure of DNA in 1953. As the method relies on diffraction and interference it requires the X-rays to be scattered coherently. When this is not the case, the incident and diffracted waves are not in phase, and X-ray imaging methods cannot generate the diffractive patterns needed to reconstruct the arrangement of the atoms in a crystal. This poses a big limit to coherent X-ray diffractive imaging since incoherent scattering predominates in the X-ray domain and much effort is needed to ensure coherence.

Now, this prerequisite no longer stands. Joachim von Zanthier and colleagues have demonstrated that incoherently scattered photons can be used to image tiny, complex structures (*Nat. Phys.* https://dx.doi.org/10.1038/nphys4301; 2017). Specifically, they have shown that incoherently scattered X-rays from a free-electron laser (FEL) can image 2D objects with a spatial resolution close to or even below the Abbe limit. The imaging capability in two dimensions was surprising to the researchers considering the much enlarged parameter space for the possible phase combinations used to determine the higher-order correlation functions. It allows, for example, imaging of arbitrary 2D objects on a substrate, and potentially transfers the ideas of quantum imaging from visible wavelengths to shorter wavelengths.

Credit: Macmillan Publishers Ltd

The team performed the experiment at the PG2 beamline of the Free-Electron Laser Hamburg (FLASH) at Deutsches Elektronen-Synchrotron (DESY), Hamburg. The FEL beam runs in a 10 Hz pulsed mode at 13.2 nm. It passes a monochromator and impinges on a moving diffusor. The pseudo-thermal light scattered by the diffusor is used to illuminate an object and the light passing through the object is measured by a charge-coupled device (CCD) image sensor. In the experiment, a 2D object mask, consisting of six square-cut holes in a hexagonal arrangement to mimic the carbon atoms in a benzene molecule, on the micrometre scale, was used to generate six quasi-monochromatic independently radiating incoherent sources. The researchers showed that they were able to determine the entire benzene structure based on the 10,800 single-shot speckle patterns (see image) obtained by the CCD detector.

"The requirements for the implementation — high brilliance, ultrashort excitations and high repetition rates — are well met by the FEL facility at DESY. Our next step is to apply the scheme in the hard X-ray regime to reveal structures of crystals, nanoparticles, or even single molecules at the atomic scale," said von Zanthier, who also added that the approach will likely improve structural analyses in biology and medicine.

Rachel Won

Published online: 22 December 2017
https://doi.org/10.1038/s41566-017-0080-5

News & Views, Nature Photon. 12, 6 (2018)

Reconstructed Image

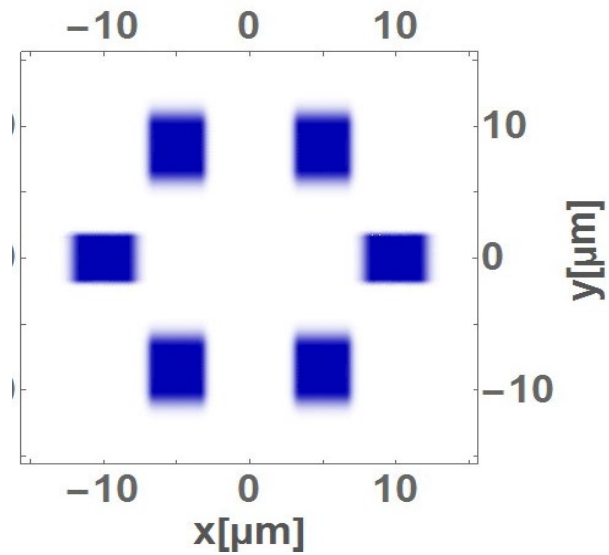

$\begin{pmatrix}3\\1\end{pmatrix}$	$\begin{pmatrix}3\\-1\end{pmatrix}$	$\begin{pmatrix}4\\0\end{pmatrix}$	$\begin{pmatrix}0\\2\end{pmatrix}$
$\begin{pmatrix}2.97\\0.97\end{pmatrix}$	$\begin{pmatrix}2.97\\-1.03\end{pmatrix}$	$\begin{pmatrix}3.90\\0.04\end{pmatrix}$	$\begin{pmatrix}0.01\\1.98\end{pmatrix}$

Schneider, Mehringer, Mercurio, Wenthaus, Classen, Brenner, Gorobtsov, Benz, Bhatti, Bocklage, Fischer, Lazarev, Obukhov, Schlage, Skopintsev, Wagner, Waldmann, Willing, Zaluzhnyy, Wurth, Vartanyants, Röhlsberger, JvZ,
Nature Phys. 14, 126 (2018)

Quantum imaging with incoherently scattered light from a Free-Electron Laser

I. Imaging with coherently diffracted vs. incoherently scattered light:

Young interference, Hanbury Brown Twiss measurement & higher order photon correlations

II. Imaging of arbitrary 1D and 2D source distributions with FLASH at XUV wavelengths using higher order photon correlations

III. Outlook: Incoherent Diffraction Imaging (IDI) of 3D atomic source distributions using hard X-rays

III. Outlook: Incoherent Diffraction Imaging (IDI)

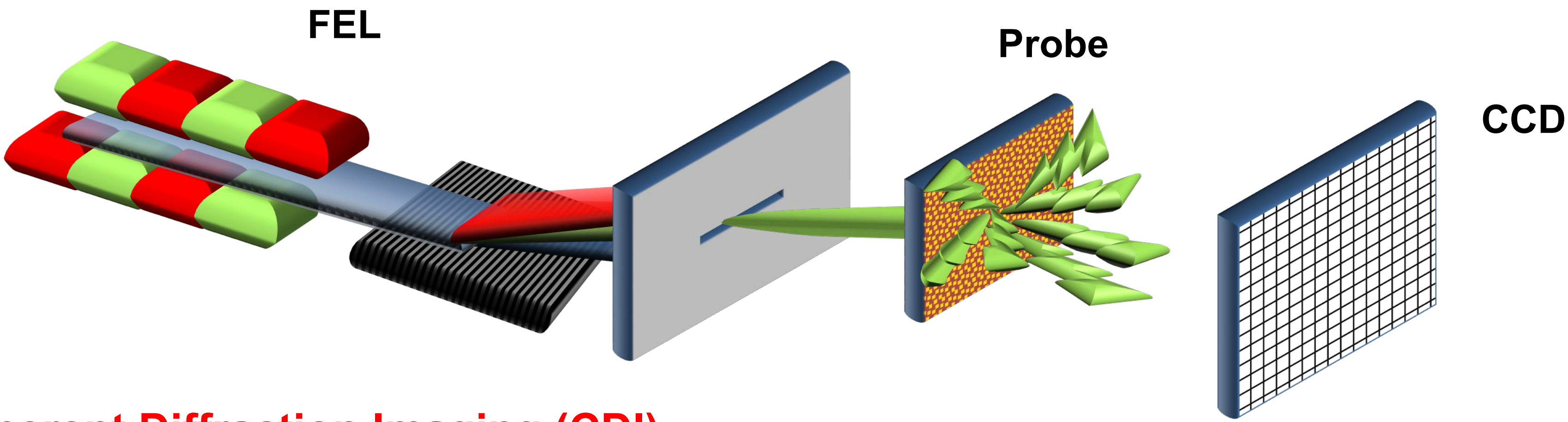

Coherent Diffraction Imaging (CDI)

Probe

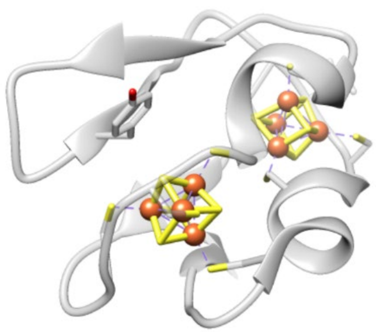

Ferredoxin (PDB: 1FDN)

Coherently diffracted light field

$$\psi(\mathbf{k}_{\text{out}}) = e^{i\mathbf{k}_{\text{in}}\cdot(\mathbf{r})} + \frac{e^{ikr}}{r} f(\mathbf{q})$$

$$f(\mathbf{q}) = -r_e \int \rho(\mathbf{r}) e^{i\mathbf{q}\cdot\mathbf{r}}\, \mathrm{d}\mathbf{r}$$

$\mathbf{q} = \mathbf{k}_{\text{out}} - \mathbf{k}_{\text{in}}$ **momentum transfer**

$\rho(\mathbf{r})$ **electron density**

III. Outlook: Incoherent Diffraction Imaging (IDI)

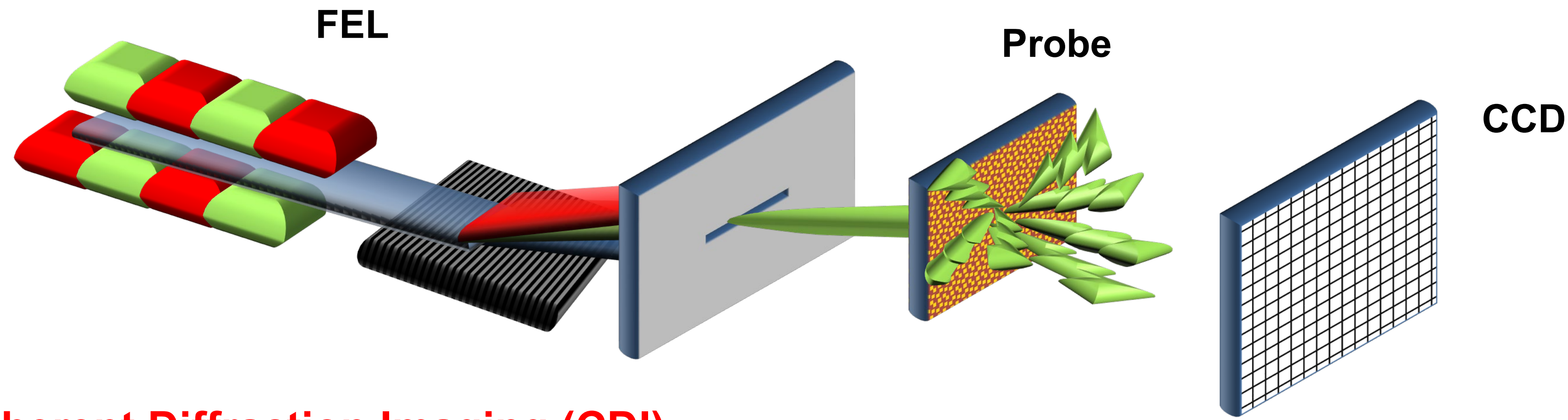

Coherent Diffraction Imaging (CDI)

Coherently diffracted light field

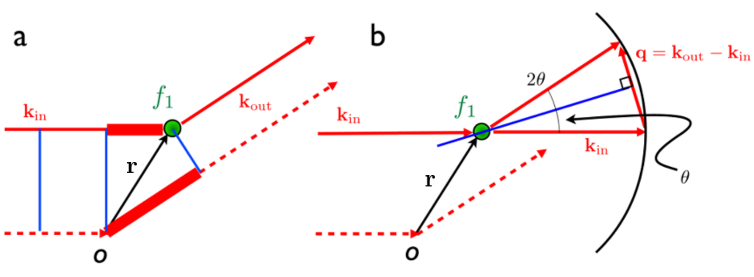

$$\psi(\mathbf{k}_{\text{out}}) = e^{i\mathbf{k}_{\text{in}}\cdot(\mathbf{r})} + \frac{e^{ikr}}{r} f(\mathbf{q})$$

$$f(\mathbf{q}) = -r_e \int \rho(\mathbf{r}) e^{i\mathbf{q}\cdot\mathbf{r}}\, \mathrm{d}\mathbf{r}$$

$$\mathbf{q} = \mathbf{k}_{\text{out}} - \mathbf{k}_{\text{in}}$$ **momentum transfer**

$$\boxed{I(\mathbf{k}_{\text{out}}) = I_0 \, |f(\mathbf{q})|^2 \, \Delta\Omega_D}$$

$$\boxed{\rho(\mathbf{r}) \sim FT^{-1}\{f(\mathbf{q})\} = \int f(\mathbf{q}) e^{-i\mathbf{q}\cdot\mathbf{r}}\, \mathrm{d}\mathbf{q}}$$

electron density

III. Outlook: Incoherent Diffraction Imaging (IDI)

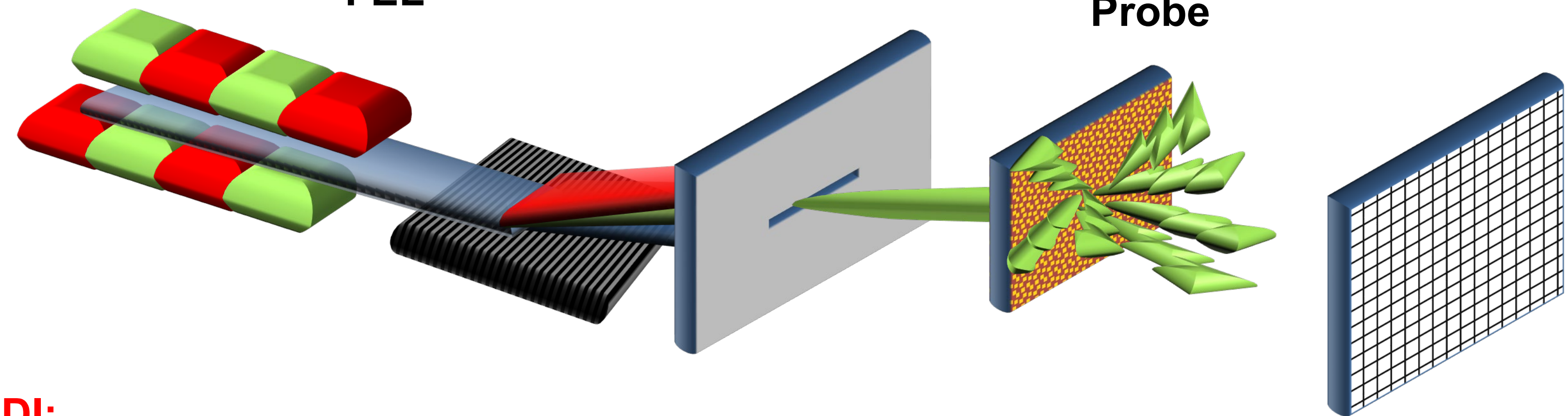

CDI:

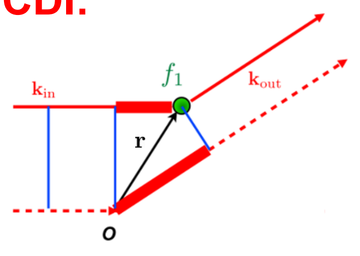

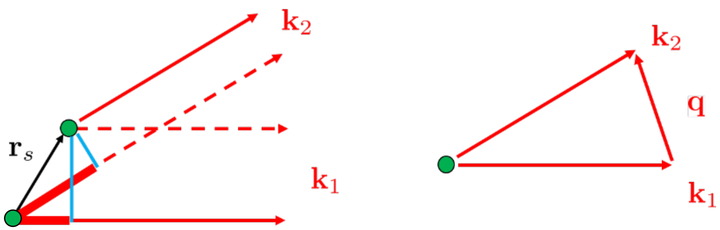

$$\mathbf{q} = \mathbf{k}_2 - \mathbf{k}_1$$

Incoherently diffracted light

$$G^{(1)}(\mathbf{k}_1) = I(\mathbf{k}_1) \;\sim\; \underline{const.}$$

$$G^{(2)}(\mathbf{k}_1, \mathbf{k}_2) \sim 1 - \frac{2}{N} + |f(\mathbf{q})|^2$$

$$\approx 1 + |f(\mathbf{q})|^2$$

$$\boxed{\rho(\mathbf{r}) \sim FT^{-1}\{f(\mathbf{q})\} = \int f(\mathbf{q}) e^{-i\mathbf{q}\cdot\mathbf{r}}\, \mathrm{d}\mathbf{q}}$$

III. Outlook: Incoherent Diffraction Imaging (IDI)

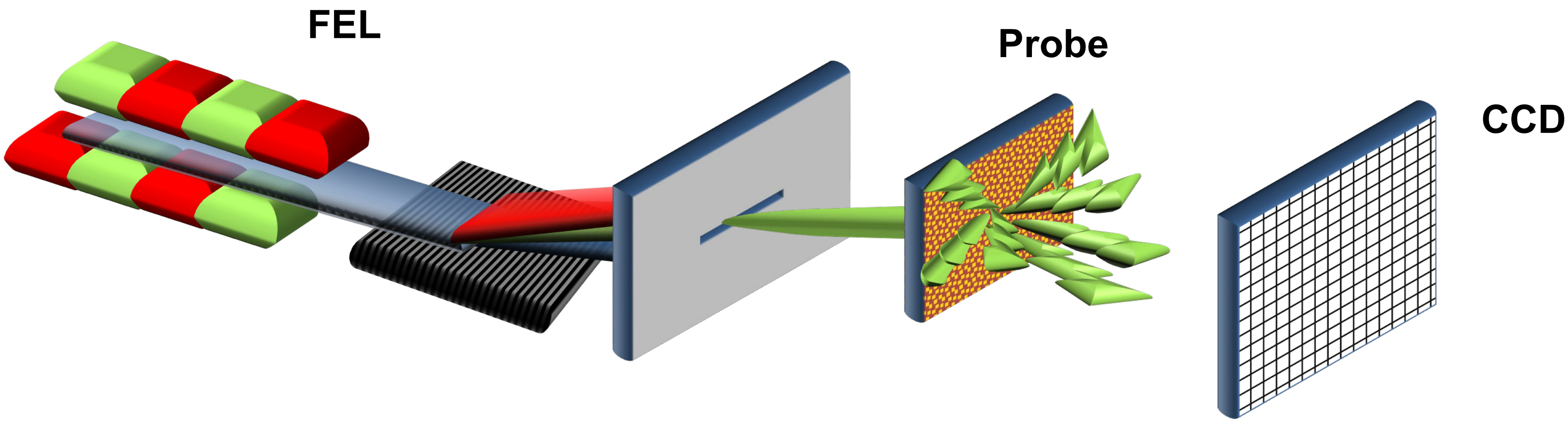

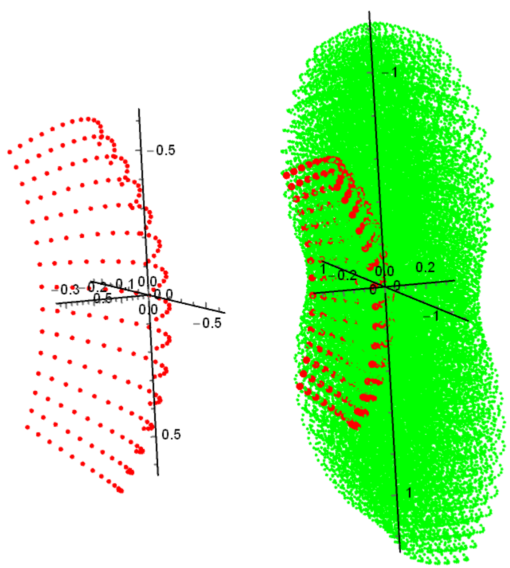

$$\mathbf{q} = \mathbf{k}_2 - \mathbf{k}_1$$

Incoherently diffracted light

$$G^{(1)}(\mathbf{k}_1) = I(\mathbf{k}_1) \ \sim \ const.$$

$$G^{(2)}(\mathbf{k}_1, \mathbf{k}_2) \ \sim \ 1 - \frac{2}{N} + |f(\mathbf{q})|^2$$

$$\approx \ 1 + |f(\mathbf{q})|^2$$

$$\boxed{\rho(\mathbf{r}) \sim FT^{-1}\{f(\mathbf{q})\} = \int f(\mathbf{q}) e^{-i\mathbf{q}\cdot\mathbf{r}}\, \mathrm{d}\mathbf{q}}$$

III. Outlook: Incoherent Diffraction Imaging (IDI)

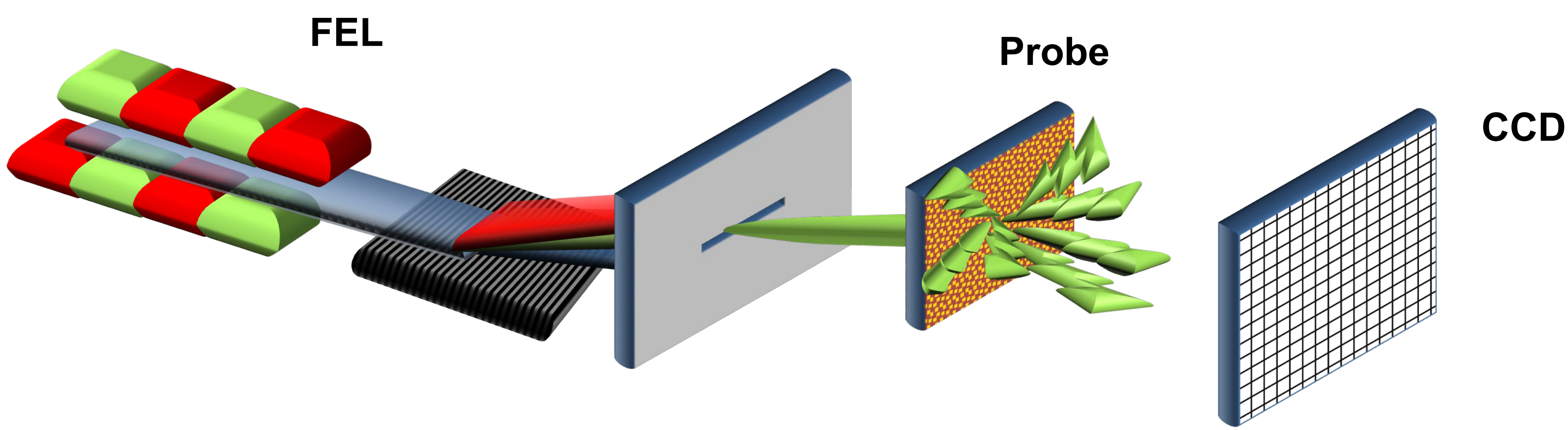

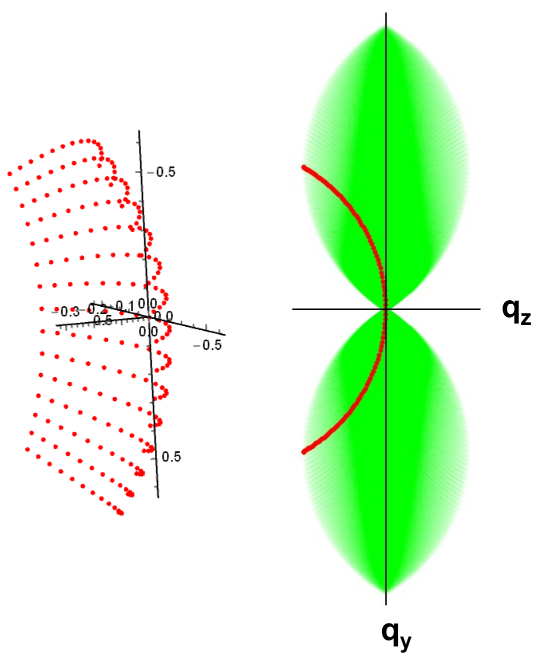

increased resolution

Incoherently diffracted light

$$G^{(1)}(\mathbf{k}_1) = I(\mathbf{k}_1) \sim const.$$

$$G^{(2)}(\mathbf{k}_1, \mathbf{k}_2) \sim 1 - \frac{2}{N} + |f(\mathbf{q})|^2$$

$$\approx 1 + |f(\mathbf{q})|^2$$

$$\boxed{\rho(\mathbf{r}) \sim FT^{-1}\{f(\mathbf{q})\} = \int f(\mathbf{q}) e^{-i\mathbf{q}\cdot\mathbf{r}}\, \mathrm{d}\mathbf{q}}$$

III. Outlook: Incoherent Diffraction Imaging (IDI)

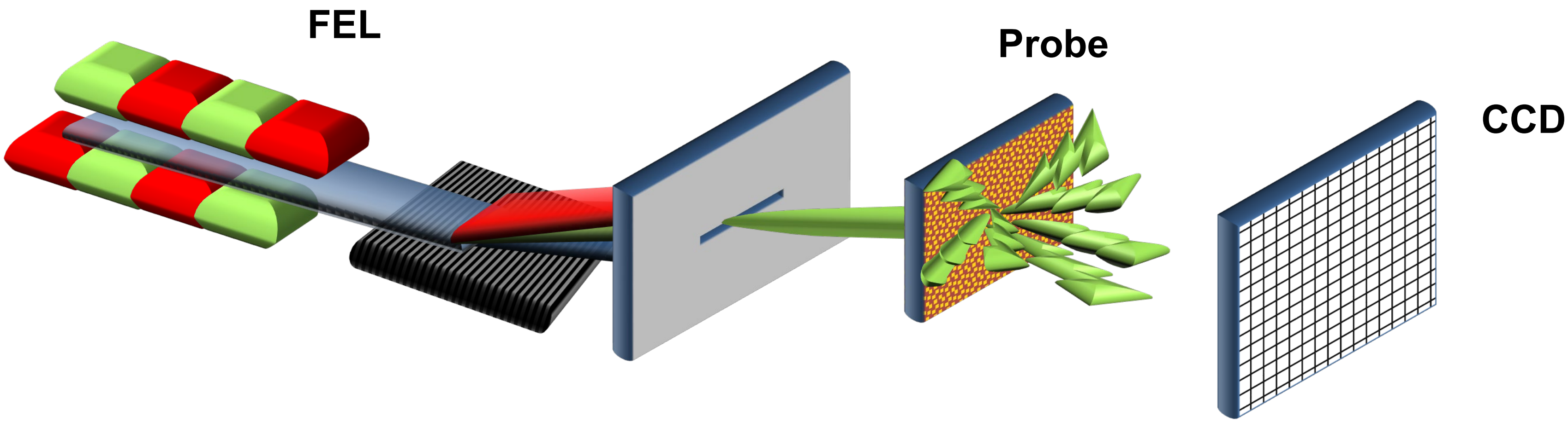

dose advantage at X-ray energies

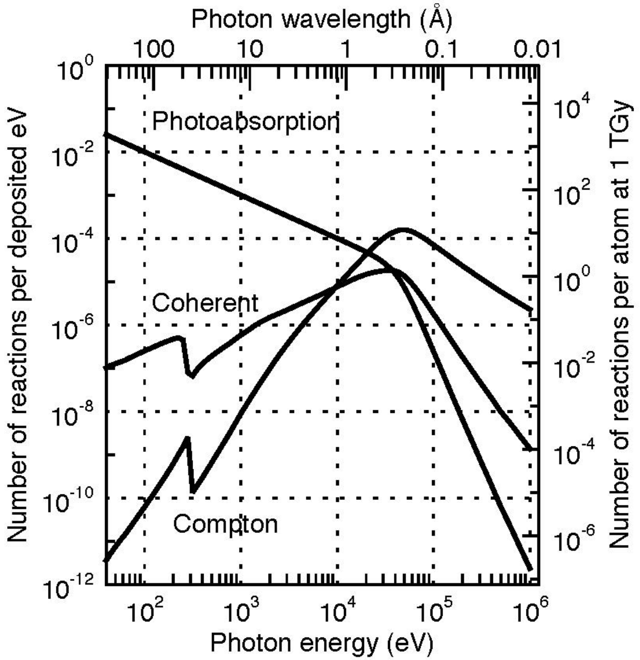

Incoherently diffracted light

$$G^{(1)}(\mathbf{k}_1) = I(\mathbf{k}_1) \sim const.$$

$$G^{(2)}(\mathbf{k}_1, \mathbf{k}_2) \sim 1 - \frac{2}{N} + |f(\mathbf{q})|^2$$

$$\approx 1 + |f(\mathbf{q})|^2$$

$$\boxed{\rho(\mathbf{r}) \sim FT^{-1}\{f(\mathbf{q})\} = \int f(\mathbf{q}) e^{-i\mathbf{q}\cdot\mathbf{r}}\, d\mathbf{q}}$$

III. Outlook: Incoherent Diffraction Imaging (IDI)

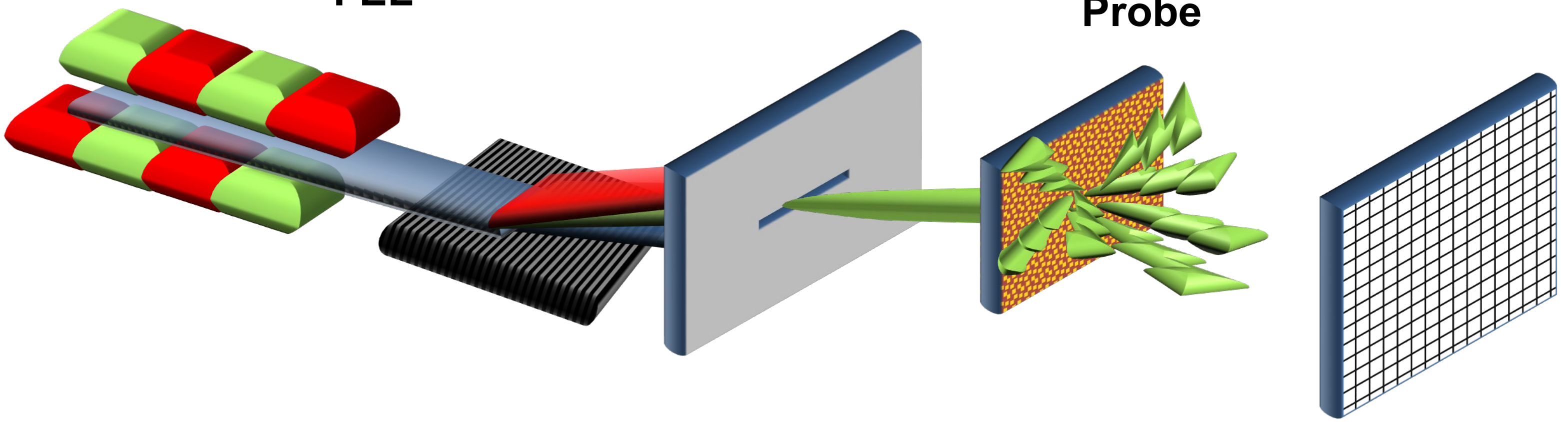

- dose advantage
- volumetric information for a single orientation
- increased resolution
- increased statistics
- element specific imaging
  - ⟷ x-ray spectroscopy

Incoherently diffracted light

$$G^{(1)}(\mathbf{k}_1) = I(\mathbf{k}_1) \sim const.$$

$$G^{(2)}(\mathbf{k}_1, \mathbf{k}_2) \sim 1 - \frac{2}{N} + |f(\mathbf{q})|^2$$

$$\approx 1 + |f(\mathbf{q})|^2$$

$$\boxed{\rho(\mathbf{r}) \sim FT^{-1}\{f(\mathbf{q})\} = \int f(\mathbf{q}) e^{-i\mathbf{q}\cdot\mathbf{r}}\, \mathrm{d}\mathbf{q}}$$

Classen, Ayyer, Chapman, Röhlsberger, JvZ, PRL 119, 053401 (2017)

III. Outlook: Incoherent Diffraction Imaging (IDI)

Improvements for Incoherent Diffractive Imaging (IDI)

- shorter pulse length of FEL (< 1 fs)

- high reprate (with detectors keeping up)

- larger detectors

- automatized evaluation (e.g., dropletization)

Conclusion and Outlook

- **Photons emitted by incoherent sources can produce diffraction patterns if measured coincidentally in the far-field (= higher order correlation functions)**

- **Arbitrary source distribution in 1D and 2D: filtering of spatial frequencies**

$$g_N^{(m)}(\delta_1) = A_0^{(m)} + \sum A_{la}^{(m)} \cdot \cos((x_l - x_a)\cdot\delta_1) \quad \textbf{if} \quad (x_l - x_a) \in \mathbb{N}_0 \cdot (m-1)$$

$$g_N^{(m)}(\delta_{1,x}, \delta_{1,y}, MP_x) = A_0 + \sum_{\substack{a,l=1\\ a\neq l}}^{N} A_{la} \cdot \begin{cases} \cos\left[(x_l - x_a)\delta_{1,x} + (y_l - y_a)\delta_{1,y}\right] & \textbf{if} \;\; (x_l - x_a) \in \mathbb{Z}\cdot(m-1) \\ 0 & \textbf{else} \end{cases}$$

using XUV light from FEL:

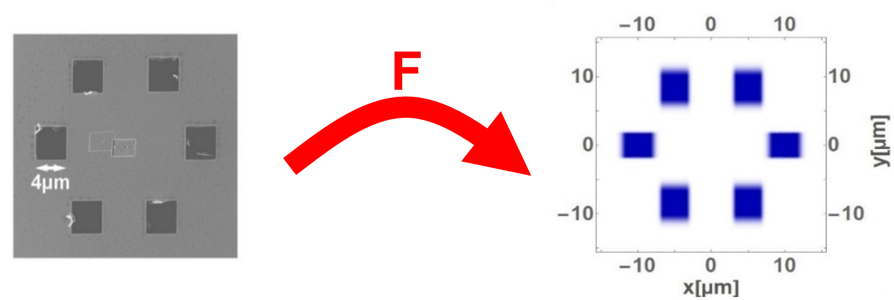

PRA 64, 063801 (2001); PRL 99, 133603 (2007); PRL 109, 233603 (2012); PRL 117, 253601 (2016)

Nature Physics 14, 126 (2018); News & Views, Nature Photonics 12, 6 (2018)

- **Incoherent Diffraction Imaging (IDI): 3D structure determination with hard x-rays**

Theory: PRL 119, 053401 (2017) **Experiment at LCLS in 2018, evaluation ongoing**

The Team:

Mona Bukenberger
Alexander Engel
Nadja Lessing
Sebastian Karl
Stephan Schuster
Valentin Klüsener

Marc Pleinert
Lukas Götzendörfer
Manuel Bojer
Stefan Richter
Anton Classen

Daniel Bhatti
Felix Waldmann
Sebastian Giebel
Christoph Biernoth
André Pscherer
Julian Wechs
Kevin Günthner
Raimund Schneider
Thomas Mehringer
Steffen Oppel
Simon Mährlein
Andreas Maser
Rico Raber
Thomas Büttner
Uwe Schilling
Ralph Wiegner
Christoph Thiel

Collaborations:

R. Röhlsberger, DESY

I. Vartanyants, DESY

W. Wurth, DESY

H. Chapman, CFEL

K. Ayyer, CFEL

J. Spence, ASU, USA

N. Zatsepin, ASU, USA

G. S. Agarwal, Texas A & M, USA

F. Schmidt-Kaler, Univ. Mainz

P. Kok, Univ. of Sheffield, UK

J. Evers, MPK, Heidelberg